Int. J. Heat Mass Transfer. Vol. 17, pp. 991–1002. Pergamon Press 1974. Printed in Great Britain

HEAT TRANSFER THROUGH A SHALLOW, HORIZONTAL CONVECTING FLUID LAYER

E. L. KOSCHMIEDER and S. G. PALLAS
College of Engineering and Center for Statistics and Thermodynamics,
The University of Texas, Austin, Texas, U.S.A.

(*Received* 9 *September* 1973 *and in revised form* 3 *January* 1974)

Abstract—The heat transfer through a shallow, horizontal, circular fluid layer, heated uniformly from below and cooled uniformly from above, has been measured. The lid of the silicone oil layer was a sapphire crystal which permitted visual observation of the flow during the heat-transfer measurements. A pattern of circular concentric rolls formed at the critical Rayleigh number. This pattern persisted to about 6 R_c, to be replaced by an irregular pattern at high R and an unsteady irregular pattern at very high Rayleigh number. The heat flux measurements confirmed a theoretical prediction of Schlüter, Lortz and Busse concerning the initial slope of the heat-transfer curve after onset of convection. The measurements seem also to confirm recent numerical studies of Plows regarding the amount of heat transferred by convection at moderately high supercritical Rayleigh numbers. At high supercritical Rayleigh numbers the measurements did not reproduce any of the slope changes in the heat-transfer curve which have been observed by other investigators.

NOMENCLATURE

α, volume expansion coefficient [$°C^{-1}$];
κ, thermal diffusivity [$cm^2 s^{-1}$];
λ, wavelength [non-dimensional];
ν, kinematic viscosity [$cm^2 s^{-1}$];
ρ, density [$g cm^{-3}$];
σ, Prandtl number;
d, fluid depth;
g, gravitational constant [$cm s^{-2}$];
n, number of rings;
Nu, Nusselt number;
R, Rayleigh number;
R_c, critical Rayleigh number;
ΔT, temperature difference across fluid.

1. INTRODUCTION

SINCE the classical study of Bénard [1] of the motions of a shallow fluid layer heated uniformly from below, the heat transfer through a convecting horizontal fluid layer has been measured repeatedly. The most notable modern study of heat transfer by Bénard convection is probably Silveston's [2] investigation. Using a technique introduced by Schmidt and Milverton [3], Silveston determined the critical Rayleigh number R_c as well as a heat-transfer curve ranging from subcritical Rayleigh numbers $R \cong 400$ to highly supercritical Rayleigh numbers $R \cong 10^6$. In the timespan since Silveston's work, Bénard convection has been studied intensively, both experimentally and theoretically. A survey of the present knowledge of Bénard convection can be found in [4]. The modern theoretical and experimental investigation make it necessary to refine Silveston's measurements. The experiments described in the following are concerned with three aspects of the heat transfer by convection, namely (a) the dependence of the heat flux on the pattern of the flow, (b) the correlation of the heat flux with the wavelength of the convective motions and, (c) the existence of slope changes in the heat-transfer curve for highly supercritical Rayleigh numbers.

The theory of finite amplitude convection of Schlüter, Lortz and Busse [5] presents formulas for the initial slope of the convective heat transport by rolls as well as by square cells and hexagons. The formulas of Schülter, Lortz and Busse refer to convective flow under a rigid lid; surface tension is therefore eliminated. Note, that the hexagonal pattern which appeared in Bénard's and several subsequent experiments were caused by surface tension effects, as was shown experimentally by Block [6] and explained theoretically by Pearson [7] and in particular by Nield [8]. Convective motions on a plane of infinite horizontal extent with rigid–rigid boundary conditions should appear in form of straight, parallel rolls, as has likewise been shown by Schlüter, Lortz and Busse [5]. In bounded containers the form of the convective motion is determined by the shape of the lateral walls, as was shown experimentally by Koschmieder [9]. In particular, a circular lateral wall causes a pattern of circular concentric rolls. An extensive theoretical study of the convective motions in a circular cylindrical fluid layer has been made by Charlson and Sani [10]. There is a number of measurements of the initial slope of the heat transfer in the literature, but none of these measurements has been made with a defined uniform flow pattern. Measurements of the initial slope of the convective heat transfer by a perfect pattern of circular concentric rolls will be described later in this paper.

There is a number of numerical investigations of the heat transfer by convection at moderately high Rayleigh numbers. The early studies have been summarized by Schneck and Veronis [11]. They note that the computations predict heat fluxes which exceed the measured heat fluxes by about 5 per cent, which seems to be outside of the error margin of the measurements. Recent computations by Lipps and Somerville [12] and Plows [13] show that the discrepancy between the computed heat transfer and the measured heat transfer vanishes if the wavelength, i.e. the size of the rolls, of the convective motions is increased with increasing Rayleigh number. Evidence for an increase of the wavelength comes from several experiments, for detail see [4]. Simultaneous measurements of the heat transfer and the wavelength of convective motions will be presented later in this paper.

There is a number of experimental investigations which indicate the existence of slope changes in the heat-transfer curve at higher Rayleigh number. There is, of course, the first "break" of the heat-transfer curve at the onset of convection, when molecular conduction is supplemented by convection. The first observation of a second break at a higher Rayleigh number has been made by Schmidt and Saunders [14]. They observed a transition to "turbulence" at $R \simeq 45\,000$ with a corresponding change in the heat transfer. Since their apparatus was not very sophisticated this observation is probably not significant. In time-dependent experiments Malkus [15] observed seven slope changes at $R = 1700 \pm 80$, $18\,000 \pm 1000$, $55\,000 \pm 4000$, $170\,000 \pm 15\,000$, $425\,000 \pm 20\,000$, $860\,000 \pm 30\,000$, and $1\,700\,000$. It appears that his data could as well be fitted by smooth curves, within the error interval of his measurements. The second slope change, for example, appeared only on three out of eight measurements at $R = 18\,000$, while the others appeared at either $11\,000 \pm 2000$ or $26\,000 \pm 5000$. In a subsequent paper Malkus [16] presented a theoretical explanation of his measurements. Each slope change is attributed to the appearance of a higher mode with wavelengths in the order of 1/2, 1/3, 1/4 etc. of the original wavelength. The Rayleigh numbers of the slope changes observed by him agree within 10 per cent with the Rayleigh numbers which follow from his theory for the appearance of the higher modes. It must be noted though that his theory is based on the existence of a mean linear temperature gradient in the fluid layer. It is, however, known from measurements of Somerscales and Dropkin [17], interferometric measurements of Gille [18] and computations of Plows [13] that the horizontally averaged temperature distribution in a supercritical convecting fluid layer is curved, with strong thermal boundary layers on top and bottom. It must also be considered that supercritical convective motions activate definitely longer wavelengths as mentioned above, instead of the shorter wavelengths which Malkus' theory studies.

A time-dependent investigation of Willis and Deardorff [19] confirmed, but renumbered, the observations of Malkus with fluids of different Prandtl number. They find slope changes at $R = 1750$, 8200, 24 000, 56 000, 180 000, 410 000, 830 000, $1{\cdot}4 . 10^6$ and $2{\cdot}25 . 10^6$. Again the evidence for the slope changes is marginal, which is particularly true for the four slope changes with the highest Rayleigh numbers. They appear to be on one smooth curve, see Fig. 4 of Willis and Deardorff. This curve presents the results of just one experiment. Note also that the choice of $Nu \times R$ as ordinate stretches the ordinate and reduces the curvature of the heat-transfer curve, which then might appear to be composed of a couple of straight sections.

There are other indications for the existence of slope changes. For example Silveston's [2] heat-transfer curve has a break near $R = 3 \times 10^5$. However, the scatter of the data (± 15 per cent) at this Rayleigh number makes it possible to draw as well a smooth curve through his measurements. No break in the heat-transfer curve appears in his measurements for Rayleigh numbers $R < 3 \times 10^5$. Di Frederico and Foraboschi [20] measured the heat transfer through a water layer cooled by evaporation. They observed a slope change at $R = (2{\cdot}2 \pm 0{\cdot}4) \times 10^4$. In time-independent experiments Krishnamurti [21, 22] found slope changes at $R = 20\,300$, $R = 59\,000$ and $R = 179\,000$. However, the straight lines which are drawn through her data seem to be arbitrary. The second and fourth break observed by her can obviously be eliminated by smooth curves which fit the data actually better or are at least within the error margin of the measurements. Ahlers [23] made measurements of the convective heat transfer in helium layers at temperatures between 2 and 5°K. He found, up to 150 R_c, only one observable singularity in the heat-transfer curve, namely the one at R_c.

Numerical investigations of Deardorff [24] and Plows [25] of the heat transfer by convection with Rayleigh numbers up to about 22 000 do not indicate the existence of slope changes. These calculations are based on flow in two-dimensional rolls with cross sections independent of Rayleigh number. The later computations of Plows [13] study the heat transfer by rolls with variable cross sections. They do not indicate slope changes either. Note, however, that Lipps and Somerville [12] could obtain realistic values of the wavelength only with three-dimensional convective flow, as distinct from the above mentioned studies which investigate two-dimensional flow. Summarizing we note that the evidence for the slope changes in the heat-transfer curve is uncertain and contradictory. New measurements of the convective heat transfer at higher Rayleigh numbers are necessary to clear up the discrepancies.

2. DESCRIPTION OF THE APPARATUS

A schematic section through the apparatus is shown in Fig. 1. The bottom of the fluid layer was a 2-in thick copper plate of 7-in dia. The copper plate was heated electrically from below with a Nicrom resistance wire in a spiral groove in a brass plate which was soldered to the copper block. The entire bottom block

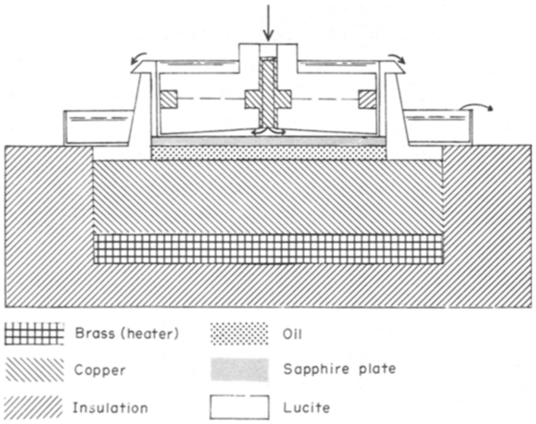

FIG. 1. Section through the apparatus.

was insulated laterally with a press fit styrofoam ring 2-in thick. The entire thickness of the copper plate was machined to within 0·001 in and the top polished to a near mirror finish. The fluid was confined laterally by a lucite ring, the inner diameter of which was 5·3125 in. The upper boundary of the fluid was a colorless monocrystal sapphire plate of 5·25-in dia. and 0·2-in thickness with a maximal variation in thickness of 0·001 in. The sapphire was obtained from Union Carbide Corporation—Electronics Division. The expensive sapphire served two purposes. First, it was transparent, so the fluid motion could be observed visually and the wavelength of the convective flow be determined. Second, the sapphire provided an upper fluid boundary of excellent thermal conductivity. Most theoretical studies of convection make the simplifying assumption of excellent thermal conductivity in the boundaries. According to the manufacturer the thermal conductivity of the sapphire is 0·088 cal/cm s°C at 25°C. This is nearly a tenth of the thermal conductivity of copper, thirty times better than the conductivity of glass and about 300 times the thermal conductivity of the silicone oils used as fluid in the experiments. The sapphire plate was cooled by water from a constant temperature bath, circulated at a rate of about 70 cm^3/s. The flow rate was monitored continuously with a Fisher and Porter flow meter. A high rate of flow is necessary to maintain a near uniform temperature on top of the convecting fluid layer. As indicated in Fig. 1 the cooling water is forced through a tube onto the center of the sapphire. From there the cooling water spreads radially under a thick lucite plate, moves upwards along a lucite cylinder which carries the sapphire, and finally runs over into a circular basin from which it is returned to the constant temperature bath.

The heat flux was determined with the help of a thermopile arrangement, measuring the temperature difference in the cooling water between the inlet pipe and the outlet of the water at the outside of the circular lucite plate that forces the water to spread uniformly over the sapphire. The thermopile consisted of ten copper–constantan thermocouples in series. Ten junctions were attached to a copper ring surrounding the input pipe. The ten alternate junctions were placed 36° apart in another copper ring at the outside of the lucite plate, as indicated in Fig. 1. This arrangement will be referred to as the heat sensor. A more detailed description can be found in Pallas [26]. The temperature difference measured with the heat sensor combined with the flow rate of the cooling water determines the heat flux through the fluid layer. There is practically no lateral heat loss from the fluid layer, since the lateral wall is made of very poorly conducting lucite and over the outer part of the lucite wall the same vertical temperature gradient as in the fluid layer is established. There is also virtually no possibility that the cooling water on its way over the sapphire looses heat upwards, before it has passed the outer copper ring. This is so since the thermopile is imbedded in lucite and the vertical temperature gradient is near nil, since the entire heat sensor is submerged in the cooling water. The heat sensor is very sensitive. Even the minute amount of heating of the cooling water which resulted from the light of a common flashlight could be detected. Temperature differences of 0·001°C between the incoming and outgoing water were routinely measured. The calibration of the heat sensor was verified with measurements in which water of known temperature passed through the center pipe, while the outer copper ring was submerged in water of a known different temperature. The emf from the thermopile was amplified and measured with a Keithley Nanovoltmeter. The temperature difference across the convecting fluid was measured with a thermocouple pair, one junction being in the center of the bottom copper plate, the other in the constant temperature bath. Both signals were recorded with a Hewlett–Packard dual track recorder. The accuracy of the nanovoltmeters was checked with a Keithley Nanovolt source.

The fluid used in the experiments was silicone oil Dow Corning 200 fluid, with viscosities ranging from 0·05 to 2 $\mathrm{cm^2/s}$. The different viscosities gave access to a wide range of Rayleigh numbers without change of the fluid depth. The silicone oil has also the advantage of a very low thermal conductivity, which for the resting fluids is around $3{\cdot}5 \times 10^{-4}$ cal/cm s°C. This, compared with the thermal conductivity of copper and the sapphire satisfies the theoretical requirement of excellent conduction in the boundaries. Furthermore, the silicone oil has the advantage of a very slow variation of the property values with temperature. For example, the fastest varying property, the viscosity, has a variation

$$\frac{1}{\nu}\frac{\partial \nu}{\partial T} = 1 \times 10^{-2}/°\mathrm{C}.$$

Accurate knowledge of the kinematic viscosity ν, thermal diffusivity κ, and of the coefficient of volume expansion α is necessary for the accurate determination of the Rayleigh number R and the Nusselt number Nu. The Rayleigh number is defined by the equation

$$R = \frac{\alpha g \Delta T d^3}{\nu\kappa}. \quad (1)$$

The Nusselt number is defined as the ratio

$$Nu = \frac{Q_{\mathrm{conv}} + Q_{\mathrm{cond}}}{Q_{\mathrm{cond}}}. \quad (2)$$

The dynamic viscosity of the fluids at various temperatures has been measured with a Brookfield synchroelectric viscometer. Values used for the density ρ, specific heat c_p and the thermal conductivity were based on data supplied by Dow Corning. The data for the thermal conductivity were verified with this apparatus using a stable temperature gradient. Details concerning the property values cannot be discussed here, but a comprehensive list can be found in the Appendix B of Pallas [26]. The fluid motions were made visible by a small amount of aluminum powder added to the fluid. Black lines in the photographs indicate places of vertical motion, bright areas indicate predominantly horizontal motion.

3. EXPERIMENTAL PROCEDURE AND CONTROLS

The experiments proceeded as follows. Oil was poured on the levelled copper plate. The fluid depth was 5·08 mm in the majority of the experiments. The sapphire was put on the fluid layer such that no air was trapped underneath. The power supply for the electric heating was set and the cooling water was circulated at a constant temperature. The time constant d^2/κ for thermal diffusion in the liquid layer was around 250 s. When the heating was increased in small steps it took around 10 min for the signals from the vertical temperature difference and the heat sensor to stabilize on the recorder. After around three times that time interval the signal obtained from the heat sensor was taken to represent the steady-state value of the heat flux. All measurements subsequently shown are steady-state measurements. Afterwards the temperature difference across the fluid layer was increased by another small step. Most experiments were repeated three or four times. Only average values of these measurements are plotted on the figures. The standard deviations of these measurements are usually within the 1 per cent range. The maximal occurring deviation was 2·4 per cent. No error bars are shown on the figures since the marks indicating the measured points are larger than the experimental errors. Also, the uncertainty in the Rayleigh number and the Nusselt number, which is mostly due to the uncertainty of the property values of the fluid, is larger than the standard deviation of the measurements. The uncertainty of the Nusselt number is due mostly to the uncertainty of the flow rate of the cooling water and the uncertainty of the thermal conductivity of the fluid, both are of order of 1 per cent. A longer analysis of the cumulative error (Pallas [26]) shows the Nusselt number to be inaccurate by ± 2 per cent. The Rayleigh number involves several property values, namely $\alpha(T)$, $\rho(T)$, $c_p(T)$, $\kappa(T)$ and $\nu(T)$. Since the Rayleigh number also incorporates the third power of the depth d of the fluid layer, even minute errors in d can contribute to the uncertainty of R. Total uncertainty in R was determined to be ± 6 per cent.

In the experiments in which the knowledge of the wavelength of the convective motions was required the wavelength was measured simultaneously with the heat flux. The nondimensional wavelength λ is the ratio of the horizontal width of two rolls divided by the fluid depth. Since the time constant for viscous dissipation d^2/ν was at most 5 s the convective flow was always in a steady state when the heat flux was steady. The nondimensional wavelength λ was determined either from the number n of the concentric rings with the formula $\lambda = r/nd$, or from actual measurements of the width of individual rings. These measurements were made on enlarged photographs of the flow pattern. In order to avoid errors due to parallax a ruler placed diagonally onto the sapphire was photographed with the pattern. Although the flow could be observed visually through the heat sensor, the heat sensor was removed for a few seconds when measurements of the wavelength or photographs of the flow were made.

A number of checks were made to verify proper functioning of the apparatus. The most simple check is a comparison of the electric heat input with the heat flux through the oil layer as measured with the heat sensor. As it turned out, 92 per cent of the heat input went through the convecting oil layer plus the lucite ring around the oil. The rest of the input heat must have been lost through the insulation surrounding the bottom plate. A second test of the apparatus was made measuring the heat flux with a positive temperature gradient. In order to do so the bottom copper plate was submerged in circulating water of constant temperature while the temperature of the water flowing through the heat sensor on top of the sapphire was gradually increased. The downward heat flux through the oil must then be a linear function of the temperature difference across the oil and the slope of that line must agree with the thermal conductivity of the oil. This was found to be the case, measured curves of the heat flux in this case can be found in Pallas [26]. Finally a check on the thermal conductivity of the sapphire was made. In order to do so the sapphire lid was replaced by a 1·73-mm thick copper plate. The heat flux through the oil in the conduction and convection range as measured with the copper plate on top of the oil was then compared with the heat flux measured while the sapphire was used for the lid. Both were found to agree perfectly, see Fig. 8. Note that with the copper plate the correction which has to be made in ΔT for the temperature drop across the copper plate is nil. Note also that the maximal correction in ΔT which had to be made for using the sapphire was 2 per cent of ΔT.

4. CONVECTIVE FLOW

The well-known hexagonal flow pattern developed on the copper bottom plate when the fluid was heated sufficiently from below and cooled by ambient air. An example of such motions is shown in Fig. 2. More regular patterns have been observed by Koschmieder [27] under thin, carefully cooled air layers. When the oil was in touch with the sapphire the fluid motions commenced at subcritical Rayleigh numbers as circular rolls along the wall, see Fig. 3(a). In these and the following pictures the outermost roll is almost completely hidden underneath the lucite cylinder which carries the sapphire. The subcritical rolls, which are caused by the presence of the lateral wall, can be maintained indefinitely if the temperature difference is maintained. Increasing ΔT caused more rolls to form, see Fig. 3(b). At R_c the entire plate was covered by thirteen concentric rings, see Fig. 3(c). When the vertical temperature difference ΔT was increased further to supercritical values the innermost ring began to shrink and disappeared when the temperature was raised sufficiently. This process continued with the consecutive disappearance of rings, see Fig. 3(d–f). At even higher Rayleigh numbers the axisymmetry of the

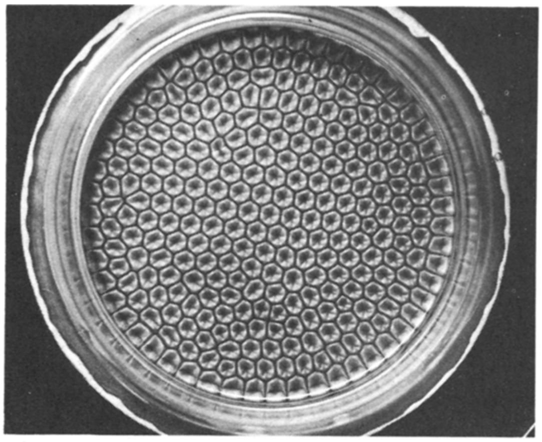

FIG. 2. Bénard cells under an air surface.

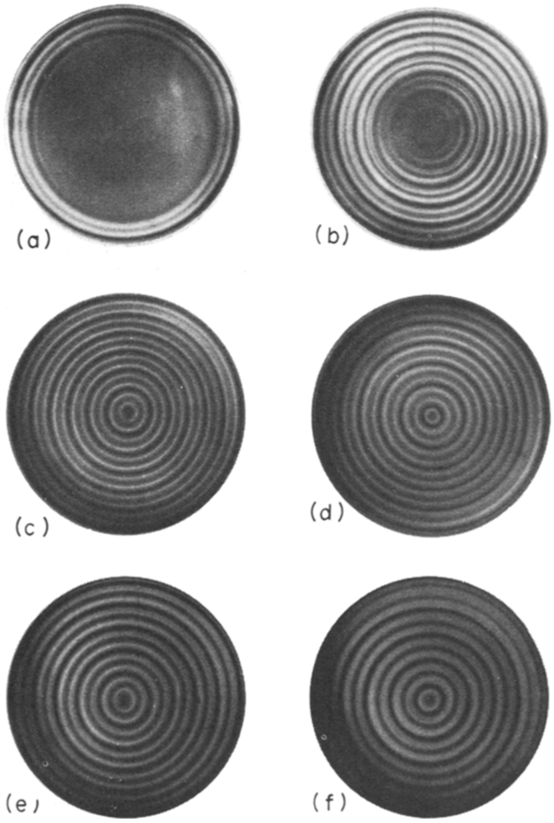

FIG. 3. Development of concentric rolls under the sapphire lid and increase of wavelength with supercritical Rayleigh number. (a) Three rolls adjacent to circular wall. $R = 0{\cdot}85\,R_c$. (b) Eleven concentric rolls. $R = 0{\cdot}95\,R_c$. (c) Thirteen circular rolls. The outermost rim roll is almost completely hidden. $R = 1{\cdot}3\,R_c$. (d) Twelve concentric rolls with shrinking center roll. $R = 2{\cdot}2\,R_c$. (e) Eleven concentric rolls just after the disappearance of the twelfth ring. $R = 3{\cdot}4\,R_c$. (f) Ten circular concentric rolls. $R = 6\,R_c$.

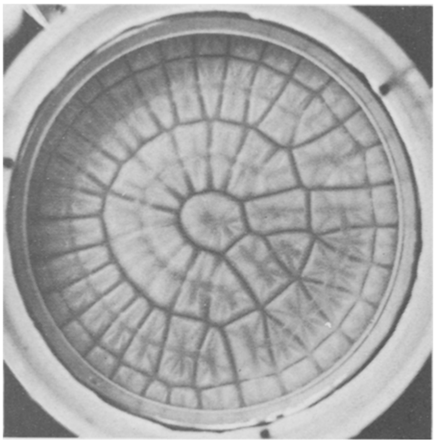

FIG. 4. Irregular laminar supercritical pattern under the sapphire lid. $R = 8\,R_c$.

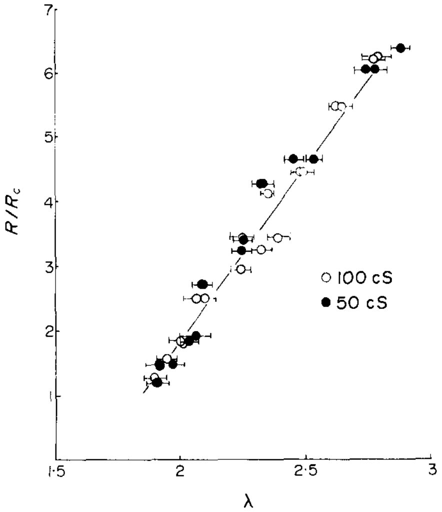

FIG. 5. Measured wavelengths as a function of Rayleigh number.

flow broke up and cells formed. First a semblance of a circular arrangement was conserved, see Fig. 4. Then, with further increases in the Rayleigh number the flow got gradually irregular and finally time-dependent.

A referee has raised the question whether the nonuniformity of the cooling caused by the presence of the lucite ring which carries the sapphire may be the cause for the continuing axisymmetry of the flow under supercritical conditions. Charlson and Sani [10] have shown that the critical energy levels for axisymmetric and nonaxisymmetric flow states are very close together, which suggests that a small nonuniformity in cooling can have a large effect on the selection of the cellular pattern. Experimental evidence seems to confirm the comment of the referee as far as the onset of convection is concerned. The pattern of circular concentric rolls appears only if utmost care is taken in providing a cooling of the lid as closely uniform as possible. The lucite support ring seems to be of little importance to the onset of convection though. A different arrangement used previously by Koschmieder [9] had a uniformly cooled lid which extended beyond the lateral rim of the fluid layer, in which case the flow pattern was likewise axisymmetric. Concerning now the question of the axisymmtery of the flow under supercritical conditions, qualitative experimental evidence shows that the flow maintains its symmetry longer if the cooling is of better uniformity. No evidence indicated that the lucite support ring influenced the supercritical flow.

Measured wavelengths of the convective motions of four experiments with the 50 cS oil ($\sigma = 511$) and 100 cS oil ($\sigma = 916$) are shown on Fig. 5. The values plotted on Fig. 5 were determined from enlarged photographs of the flow. The distance from one ring to another was measured with a comparator, which measures distances with an accuracy of 1/100 mm. The wavelengths on Fig. 5 are not the arithmetic average of the wavelength of all rings. The rim ring was discarded, since in all cases the width of the rim roll was substantially larger than the average roll. This is due to insufficient cooling of the rim roll from above. This is so, since the sapphire is covered over a large part of the rim roll with the lucite ring that carries the sapphire. The arithmetic average wavelength of the remaining rings and, in particular, the standard deviation of the average were found to be strongly affected by the size of the center ring. The center ring varied from very large, just after the disappearance of a ring, to very small just before its disappearance. The standard deviation of the arithmetic average wavelength varied therefore from 5 to 15 per cent, which is unreasonably large in view of the regularity of the pattern and the accuracy with which the width of the rings can be measured. Therefore the measured width of the rings, as well as the squares of the deviation of each ring from the average, were weighted with the ratio of the area of the ring to the area of the outermost ring. This procedure reduces the importance of the center ring. The weighted standard deviation ranged then from 2 to 5 per cent, which is in agreement with the actual accuracy of the measurement. The weighted average wavelength and the weighted error are shown on Fig. 5.

The wavelength seems to be a linear function of the Rayleigh number between $R/R_c = 1$ and $R/R_c = 6$ within the accuracy of the measurements. The average slope, which is indicated by the broken line on Fig. 5, is given by the relation.

$$\frac{\Delta\lambda}{\Delta(R/R_c)} = 0{\cdot}44 \pm 6 \text{ per cent.} \tag{3}$$

Also, the variation of the wavelength is independent of the viscosity of the oils, within the accuracy of the measurements. Note that the line connecting the points on Fig. 5 intersects the line $R/R_c = 1$ at around $\lambda = 1{\cdot}9$, while the theoretical critical wavelength is $\lambda_c = 2{\cdot}016$. This is due to the fact that an integer number of rings has to fit the container. This quantization condition permits a variation of the critical wavelength by the amount $\pm\Delta\lambda = \lambda/2n$. The points shown on Fig. 5 are just compatible with the critical theoretical wavelength within this error interval. To put this statement in another way, the fluid depth was too large to form thirteen rings with the proper width to depth ratio. Other measurements of the wavelength as a function of the Rayleigh number can be found in Silveston [2], Krishnamurti [21], and Deardorff, Willis and Somerville [28]. These measurements show also that the wavelength increases with R, but the values of λ reported here are longer than those observed by [2, 21, 28].

5. HEAT TRANSFER

The heat transfer through layers of oil of different viscosities or Prandtl number is shown on Figs. 6–10. The choice of the viscosity determines the range in Rayleigh numbers in which measurements can be made if the geometry of the apparatus, i.e. the fluid depth is to be preserved. This means that, with fluids of low viscosity, measurements cannot be made at subcritical R, since the critical temperature difference ΔT_c is then so small that the heat transfer cannot be measured accurately. On the other hand, fluids of large viscosity cannot be brought to very high Rayleigh numbers since that would require too large temperature differences. The heat flux through the $2{\cdot}00\,\mathrm{cm^2/s} = 200\,\mathrm{cS}$ oil is shown on Fig. 6. In the conduction range with $R/R_c < 1$, when convective motions are absent, the Nusselt number equals one, as it should be.

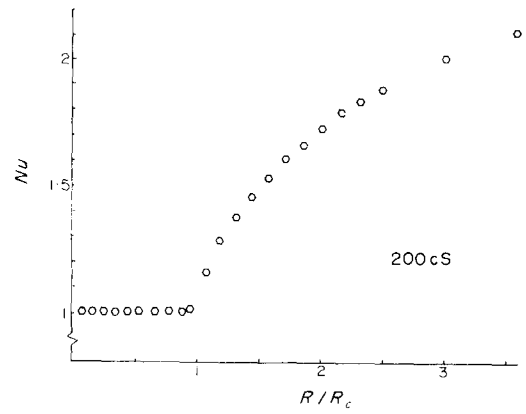

FIG. 6. Heat-transfer curve for 200 cS silicone oil.

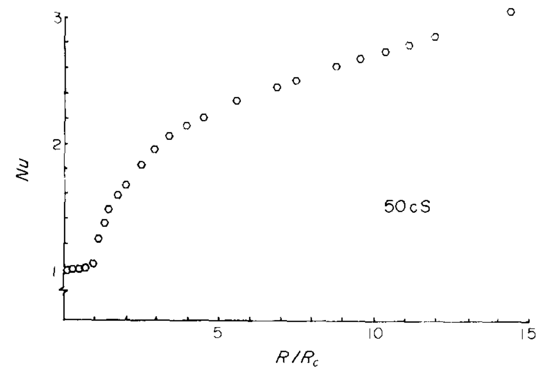

FIG. 7. Heat-transfer curve for 50 cS silicone oil.

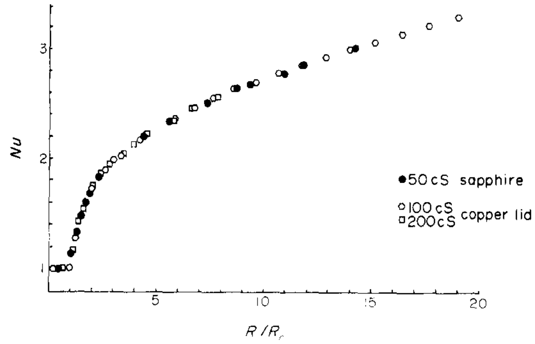

FIG. 8. Comparison of heat transfer measured with the sapphire lid with the heat transfer measured with the copper lid.

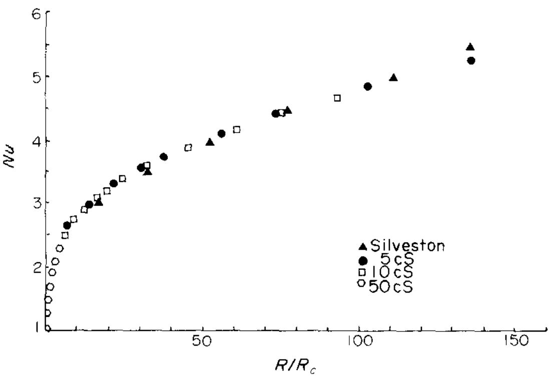

FIG. 9. Comparison of the measurements of Silveston with the measurements in the present experiments.

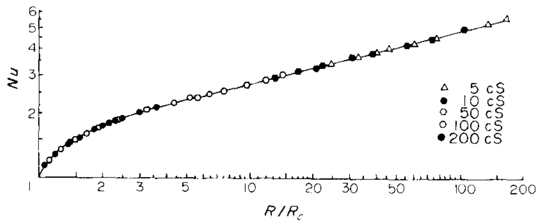

FIG. 10. Heat-transfer curve over entire range of Rayleigh numbers.

Actually, we expected a gradual increase in the Nusselt number to $Nu > 1$ as R_c was approached since subcritical motions developed from the rim. However, in none of the measurements a systematic increase of the Nusselt number was observed before the entire plate was covered with rings, that means before R_c was reached. Since the existence of the subcritical rings is undeniable, they must transport additional heat. However, it appears that the subcritical motions are so slow that the amount of heat transferred by them was too small to be picked up by the heat sensor within its accuracy. Qualitative visual observations of the motions of the aluminum tracer particles support this contention. The aluminum particles move over finite distances only after the critical Rayleigh number is exceeded. For values of $R > R_c$ the heat flux increases immediately and rapidly. Figure 6 extends only to about $3{\cdot}5\,R_c$, the vertical temperature difference across the fluid was then about 60°C and was not increased further. At $3{\cdot}5\,R_c$ the flow was still in concentric rings of perfect symmetry. The measured critical Rayleigh number for the 200 cS oil which follows from the data in Fig. 6 is listed in Table 1. The deviations from the theoretically expected $R_c = 1707$ are all within the ± 6 per cent accuracy with which the Rayleigh number is known. Table 1 lists also the corresponding results for the 100 and 50 cS oils. Figure 7 shows the measured heat transfer through the 50 cS oil. This curve extends to $15\,R_c$. The flow lost its axisymmetry at around $7\,R_c$. Measurements which compare the data obtained with the 50 cS oil with data from the 100 and 200 cS fluids are shown in Fig. 8. The viscous 100 cS and 200 cS oils are under the thin copper lid instead of the sapphire.

Table 1

Fluid viscosity cS	σ (25°C)	d (cm)	ΔT_{cr} (°C)	R_c exp	Deviation from R_c theory
50	511	0·508	6·2	1741	+2%
100	916	0·508	13·6	1630	−4%
200	1673	0·508	24·0	1675	−2%

Both sets of data agree almost perfectly. The range in Rayleigh numbers which can be reached with the viscous fluids is now larger, since the fluid depth under the copper lid was 8·33 mm.

Measurements made with the 5, 10 and 50 cS oils are shown on Fig. 9, together with points taken from Silveston [2]. The points marked Silveston do not represent actual data from his measurement but rather correspond to the curve drawn through a conglomeration of his results obtained with water, heptane and silicone oil. Agreement between his curve and our measurements seems to be satisfactory. Finally Fig. 10 shows a plot of the measurements made with all oils in the convection range from R_c to $150\,R_c$. This curve is compared with Silveston's curve and the results of Plows' [13] computations on Fig. 11. It seems to be obvious that the break in Silveston's curve at around $20\,R_c$ is not substantiated. Note that the scatter of Silveston's data at that point amounts to about 30 per cent of the Nusselt number. Otherwise the results agree

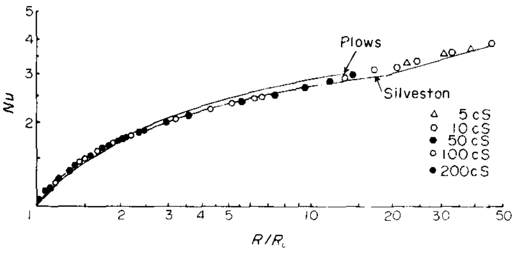

FIG. 11. Comparison of the numerical results of Plows and the measurements of Silveston with the results of the present experiments.

quite well. There is also good qualitative agreement with the results of Plows, taken from his tables IV-9 and IV-10 for fluids with $\sigma = 200$. Plows does, however, predict a heat flux slightly larger than measured here. This difference will probably vanish if the increase of the wavelength λ which Plows considers is increased further to match the increase of λ observed in our experiments.

6. THE INITIAL SLOPE, THE WAVELENGTH HEAT-TRANSFER CORRELATION AND THE SLOPE CHANGES

From the data presented in Figs. 6–10 the wanted information concerning the initial slope of the convective part of the heat-transfer curve can be obtained. The formula which Schlüter, Lortz and Busse [5] give for the initial slope of the heat flux after onset of convection in the form of rolls is

$$\frac{\bar{H}}{R-R_c} = \frac{R(Nu-1)}{R-R_c} = \frac{1}{0{\cdot}699 - 0{\cdot}0047/\sigma}, \quad (4)$$

neglecting higher order terms in the Prandtl number σ. Since the Prandtl number of the fluids used for the slope determination is larger than 500, the initial slope should be independent of σ in these measurements. Thus the slope to be expected is

$$\frac{R(Nu-1)}{R-R_c} = 1{\cdot}43. \quad (5)$$

It follows from analogous formulas that the slope for square cells should be 1·28 and for hexagons be 1·12. Using $R \times Nu$ as ordinate and R/R_c as abscissa we obtain Fig. 12. The numerator of equation (4) is equal to the distance between the full line and the dashed line which indicates the location of $R \times Nu$ when

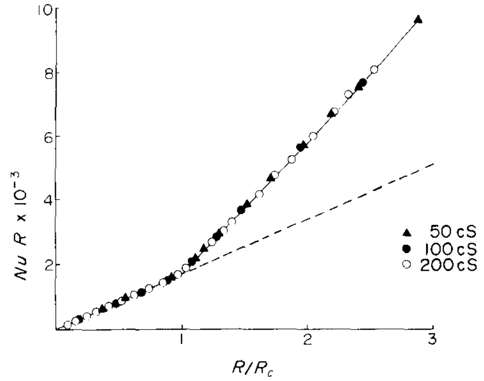

FIG. 12. Determination of the initial slope of the heat-transfer curve.

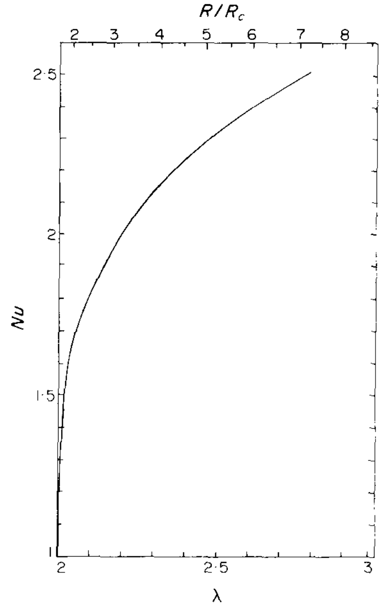

FIG. 13. The heat flux as a function of the wavelength and the Rayleigh number.

$Nu = 1$. Dividing for example at $R/R_c = 2$ the difference $R \times Nu - R$ by $R - R_c$ gives a value for the initial slope of 1·48 which is, within the error of measurement, in agreement with the theoretical prediction. The slope is also independent of σ, within the range of Prandtl numbers used. The value for the slope is clearly distinct from the slope to be expected for hexagons or square cells. This seems to be the first time that formula (4) has been verified experimentally. Note, however, that the theory concerns straight parallel rolls, while the heat flux measured here is caused by circular, concentric rolls.

The measured dependence of the heat transfer on the wavelength of the convective motions is shown on Fig. 13. The abscissa is the measured wavelength of the 50, 100 and 200 cS oils. The curve $Nu(\lambda)$ implies that the Nusselt number is very sensitive to small changes in the wavelength immediately after the onset of convection. On the other hand, the curve seems to indicate that the Nusselt number approaches independence of the wavelength as the wavelength becomes very large. Comparison of the measured data with information from numerical studies of Lipps and Somerville [12] and Plows [13] is made in Table 2. Plows computed the Nusselt number for a given fixed λ for several Rayleigh numbers. The values of Plows quoted in Table 2 were chosen such that they correspond to the minimum Rayleigh number used by Plows for a wavelength given by us. Plows' results can be probably brought into better agreement with our measurements if the wavelength in his computations is increased further.

Finally the question of the slope changes at higher Rayleigh number. The data for the supercritical heat flux are plotted on Fig. 14(a–c), using as ordinate the nondimensional heat flux $Nu \times R$, as is customary in investigations which study the slope changes. The entire range from R_c to $170\,R_c$ has been broken up into three sections, so that each section overlaps a region in which a slope change is expected. Figure 14(a) covers the region around $R = 8200 \cong 4{\cdot}8\,R_c$, where the first slope change was observed by Willis and Deardorff [18]. Within the accuracy of our measurements we cannot find a slope change, for three different oils and the 100 cS fluid also under the copper lid. The range between $5\,R_c$ and $20\,R_c$ shown on Fig. 14(b) should

Table 2

	Nusselt number			Wavelength			Relative deviation	
R/R_c	Plows	L & S	Present	Plows	L & S	Present	Nusselt (%)	Wavelength (%)
2·928	2·094		1·95	2·1		2·16	7	2·8
3·513	2·219	2·22	2·09	2·2	2·2	2·26	6·6	2·5
4·099	2·316		2·15	2·3		2·32	7·5	1
5·270	2·474		2·32	2·4		2·5	6	0·5
7·027	2·650	2·58	2·5	2·5	2·8	2·72	6·1	9·3

cover the slope change at $R = 24\,000 \cong 14\,R_c$ of Willis and Deardorff, the slope change at $R = 18\,000 \cong 10{\cdot}6\,R_c$ of Malkus [15] and the slope change at $13\,R_c$ of Krishnamurti [21]. Again the data from our measurements for three different oils seem to be on one smooth, gently curved line. Finally the range between $25\,R_c$ and $170\,R_c$ should show slope changes at around $33\,R_c$ and $100\,R_c$ according to Malkus, Willis and Deardorff, and Krishnamurti. Within the accuracy of our measurements the heat flux as plotted on Fig. 14(c) seems to be a smooth curve as well.

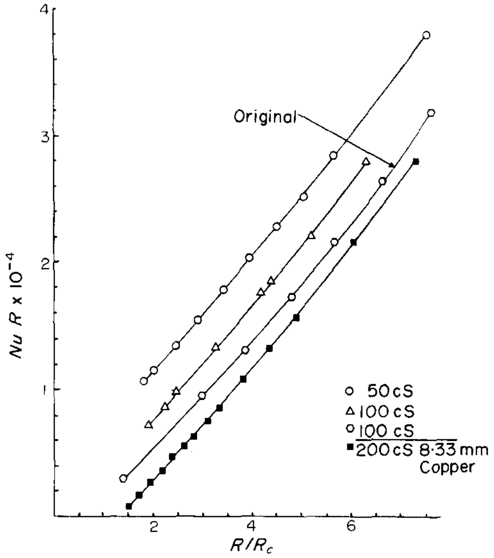

(a)

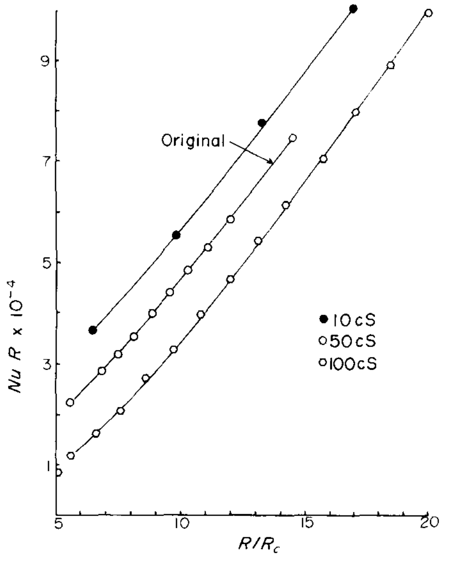

(b)

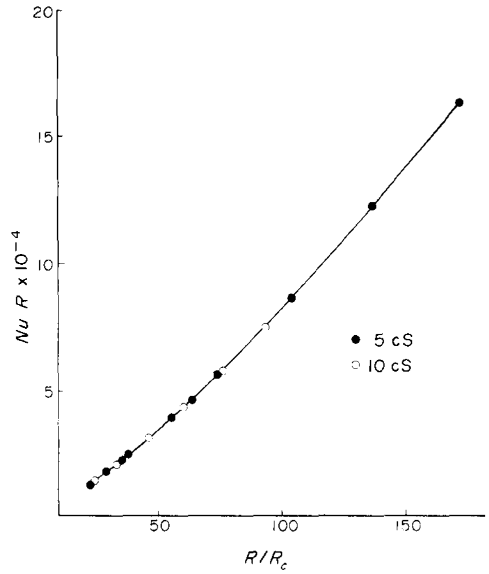

(c)

FIG. 14. Search for slope changes in the heat-transfer curve. Measured points of different sets of experiments have been shifted from the curve marked "original" to avoid crowding of the points. (a) Heat flux vs Rayleigh number. $R < 8\,R_c$. (b) Heat flux vs Rayleigh number. $R < 20\,R_c$. (c) Heat flux vs Rayleigh number. $R < 170\,R_c$.

7. CONCLUSIONS

The measurements of the heat transfer through a shallow convecting fluid layer confirm positively the value of the initial slope of the convective heat transfer of a roll pattern predicted theoretically by Schlüter, Lortz and Busse [5]. The initial slope was found to be independent of the Prandtl number for the high Prandtl number fluids used, in agreement with theory. The critical Rayleigh number measured was found to agree with the theoretically predicted, within a ± 6 per cent error of the Rayleigh number. The limiting factor in the accuracy of the Rayleigh number is the accuracy with which the fluid properties are known. The measurements of the heat transfer up to around $20\,R_c$ seem to be in reasonable agreement with the heat transfer predicted numerically by Lipps and Somerville [12] and by Plows [13]. If these studies had used longer wavelengths than they actually have, then the computed and our measured heat transfer would probably have matched. Within the range of Prandtl numbers used, no dependence of the heat transfer on the Prandtl number was apparent in the measurements. This agrees with the results of Plows [13] studies, which indicate a dependence of the heat transfer on σ only for Prandtl numbers smaller than 10, while the minimal σ used in our measurements was 50. The search for slope changes in the heat-transfer curve at high supercritical Rayleigh numbers was in vain. Within the accuracy of our measurements the heat transfer curve for supercritical Rayleigh numbers seems to be a smooth curve without slope changes up to $170 R_c$. This does, of course, not exclude the existence of any slope change at all. But it indicates that the slope changes observed by other investigators may originate from time-dependent operation of the apparatus or as seems more likely, from the scatter of the data which permits to draw linear sections of the heat-transfer curve. Further search for slope changes would be justified if solid theoretical evidence indicates the existence of such slope changes. However, the theoretical understanding of supercritical Bénard convection extends at present at most to Rayleigh numbers a few times critical.

Acknowledgements—This work was supported in part by NSF Grant GA-11484. Work of S. G. Pallas was done in partial fulfillment of the requirements of a Ph.D. degree.

REFERENCES

1. H. Bénard, Les tourbillons cellulaire dans une nappe liquide, *Revue Gen. Sci. Pur. Appl.* **11**, 1261–1271 (1900).
2. P. L. Silveston, Wärmedurchgang in waagerechten Flüssigkeitsschichten, *Forsch. Geb. IngWes.* **24**, 29–32, 59–69 (1958).
3. R. J. Schmidt and S. W. Milverton, On the instability of a fluid when heated from below, *Proc. R. Soc.* **A152**, 586–594 (1935).
4. E. L. Koschmieder, Bénard convection, *Adv. Chem. Phys.* **26**, 177–212 (1973).
5. A. Schlüter, D. Lortz and F. Busse, On the stability of steady finite amplitude convection, *J. Fluid Mech.* **23**, 129–144 (1965).
6. M. J. Block, Surface tension as the cause of Bénard cells and surface deformation in a liquid film, *Nature, Lond.* **178**, 650–651 (1956).
7. J. R. A. Pearson, On convection cells induced by surface tension, *J. Fluid Mech.* **4**, 489–500 (1958).
8. D. A. Nield, Surface tension and buoyancy effects in cellular convection, *J. Fluid Mech.* **19**, 341–352 (1964).
9. E. L. Koschmieder, On convection on a uniformly heated plane, *Beitr. Phys. Atmos.* **39**, 1–11 (1966).
10. G. S. Charlson and R. L. Sani, Thermoconvective instability in a bounded cylindrical fluid layer, *Int. J. Heat Mass Transfer* **13**, 1479–1496 (1970).
11. P. Schneck and G. Veronis, Comparison of some recent experimental and numerical results in Bénard convection, *Physics Fluids* **10**, 927–930 (1967).
12. F. B. Lipps and R. C. J. Somerville, Dynamics of variable wavelength in finite-amplitude Bénard convection, *Physics Fluids* **14**, 759–765 (1971).
13. W. H. Plows, Numerical studies of laminar, free convection in a horizontal fluid layer heated from below, Ph.D. thesis, University of California/Livermore (1972).
14. R. J. Schmidt and O. A. Saunders, On the motion of a fluid heated from below, *Proc. R. Soc.* **A165**, 216–228 (1938).
15. W. V. R. Malkus, Discrete transitions in turbulent convection, *Proc. R. Soc.* **A225**, 185–195 (1954).
16. W. V. R. Malkus, The heat transport and spectrum of thermal turbulence, *Proc. R. Soc.* **A225**, 196–212 (1954).
17. E. F. C. Somerscales and D. Dropkin, Experimental investigation of the temperature distribution in a horizontal layer of fluid heated from below, *Int. J. Heat Mass Transfer* **9**, 1189–1204 (1966).
18. J. Gille, Interferometric measurement of temperature gradient reversal in a layer of convecting air, *J. Fluid Mech.* **30**, 371–384 (1967).
19. G. E. Willis and J. W. Deardorff, Confirmation and renumbering of the discrete heat flux transitions of Malkus, *Physics Fluids* **10**, 1861–1866 (1967).
20. J. DiFederico and F. P. Foraboschi, A contribution to the study of free convection in a fluid layer heated from below, *Int. J. Heat Mass Transfer* **9**, 1351–1360 (1966).
21. R. Krishnamurti, On the transition to turbulent convection. Part 1. The transition from two- to three-dimensional flow, *J. Fluid Mech.* **42**, 295–307 (1970).
22. R. Krishnamurti, On the transition to turbulent convection. Part 2. The transition to time-dependent flow, *J. Fluid Mech.* **42**, 309–320 (1970).
23. G. Ahlers, Convective heat transport between horizontal parallel plates, *Bull. Am. Phys. Soc.* **17**, 59 (1972).
24. J. W. Deardorff, Examination of numerically calculated heat fluxes for evidence of a supercritical transition, *Physics Fluids* **11**, 1254–1256 (1968).
25. W. H. Plows, Some numerical results for two-dimensional steady laminar Bénard convection, *Physics Fluids* **11**, 1593–1599 (1968).
26. S. G. Pallas, Heat transfer and wavelength measurement for axisymmetric flow of a fluid heated from below, Ph.D. thesis, University of Texas, Austin (1972).
27. E. L. Koschmieder, On convection under an air surface, *J. Fluid Mech.* **30**, 9–15 (1967).
28. G. E. Willis, J. W. Deardorff and R. C. J. Somerville, Roll-diameter dependence in Rayleigh convection and its effect upon the heat flux, *J. Fluid Mech.* **54**, 351–367 (1972).

TRANSFERT THERMIQUE A TRAVERS UNE MINCE COUCHE HORIZONTALE DE FLUIDE

Résumé– On mesure le transfert thermique à travers une couche de fluide mince, horizontale, circulaire, chauffée à la base et refroidie uniformément sur le dessus. Le couvercle au dessus de la couche d'huile de silicone est un cristal de saphir qui permet des visualisations durant les mesures. Une configuration de rouleaux circulaires concentriques se forme au nombre de Rayleigh critique. Cette figure persiste jusqu'à $6R_c$ environ, pour être remplacée aux nombres R élevés par une configuration irrégulière et ensuite par une autre instable et irrégulière, aux très grands nombres de Rayleigh. Les mesures confirment les prédictions de Schlüter, Cortz et Busse concernant la pente initiale de la courbe de transfert thermique après l'établissement de la convection. Les mesures semblent aussi confirmer les calculs numériques récents de Plows sur la quantité de chaleur transférée par convection, pour les valeurs modérément supercritiques du nombre de Rayleigh. Aux fortes valeurs supercritiques, les mesures ne reproduisent pas les changements de pente de la courbe de transfert thermique, observés par d'autres expérimentateurs.

WÄRMEDURCHGANG DURCH EINE FLACHE, HORIZONTALE, WÄRMEÜBERTRAGENDE FLÜSSIGKEITSSCHICHT

Zusammenfassung—Es wurde der Wärmedurchgang durch eine flache, waagerechte, kreisförmige Flüssigkeitsschicht gemessen, die von unten gleichmäßig geheizt und von oben gleichmäßig gekühlt wurde.

Die obere Abdeckplatte der Siliconölschicht war ein Saphir-Kristall, wodurch eine visuelle Beobachtung während der Wärmeübertragungsmessungen möglich war. Bei der kritischen Rayleigh-Zahl bildet sich ein Muster von konzentrischen Wirbelwalzen. Dieses Muster war bis ungefähr $6Ra_{krit}$ beständig, wandelte sich zu einem unregelmäßigen Muster bei hohen und zu einem unstetigen und unregelmäßigen Muster bei sehr hohen Werten der Rayleigh-Zahl.

Die Wärmestrommessungen bestätigten, was die Anfangssteigung der Wärmeübergangskurve nach dem Einsetzen der Konvektion anbetrifft, eine theoretische Voraussage von Schlüter, Lortz und Busse. Die Messungen scheinen außerdem die Ergebnisse neuerer numerischer Studien von Plows zu bestätigen, die sich auf die bei mäßig hohen, überkritischen Rayleigh-Zahlen übertragene Wärme beziehen. Bei hohen, überkritischen Rayleigh-Zahlen erbrachten die Messungen keine der von anderen Forschern beobachteten Steigungs änderungen der Wärmeübergangskurve.

ПЕРЕНОС ТЕПЛА ЧЕРЕЗ ТОНКИЙ ГОРИЗОНТАЛЬНЫЙ КОНВЕКТИВНЫЙ СЛОЙ ЖИДКОСТИ

Аннотация — Измерялся перенос тепла через тонкий горизонтальный цилиндрический слой жидкости, равномерно нагреваемый снизу и равномерно охлаждаемый сверху. Верхней границей слоя селиконового масла служил сапфировый кристалл, что позволяло визуализировать течение при расчете теплообмена. При критическом числе Релея наблюдалась конвекция в виде круговых коаксиальных валов. Эта структура сохранялась до $6R_c$, заменялась структурой геометрически неправильной формы при большом R и неустойчивой структурой геометрически неправильной формы при очень большом числе Релея. Измерения теплового потока подтвердили теоретические расчёты начального наклона кривой теплообмена после возникновения конвекции, проведенные Шлютером, Лорцем и Буссе. Оказывается, что измерения также подтверждают результаты недавно проведенных численных исследований Плоуза о конвективном переносе тепла в потоке при не очень высоких сверхкритических числах Релея. При высоких сверхкритических числах Релея измерения не воспроизводят каких-либо изменений наклона кривой теплообмена, которые наблюдались другими исследователями.